Inorg. Chem. **2007**, *46*, 1603–1611

Blue Phosphorescence from Mixed Cyano–Isocyanide Cyclometalated Iridium(III) Complexes

Kenneth Dedeian,* Jianmin Shi, Eric Forsythe, and David C. Morton

Army Research Laboratory, 2800 Powder Mill Road, Adelphi, Maryland 20783

Peter Y. Zavalij

Department of Chemistry and Biochemistry, University of Maryland, College Park, Maryland 20742

Received August 10, 2006

The synthesis, structure, and photophysical and electrochemical properties of cyclometalated iridium complexes with ancillary cyano and isocyanide ligands are described. In the first synthetic step, cleavage of dichloro-bridged dimers $[Ir(N\hat{}C)_2(\mu\text{-}Cl)]_2$ (N^C = 2-phenylpyridine, 2-(2-fluorophenyl)pyridine, and 2-(2,4-difluorophenyl)pyridine) by isocyanide ligands gave monomeric species of the types $Ir(N\hat{}C)_2(RNC)(Cl)$ (RNC = *t*-butyl isocyanide, 1,1,3,3-tetramethylbutyl isocyanide, 2-morpholinoethyl isocyanide, and 2,6-dimethylphenyl isocyanide). In turn, the chloride was replaced by cyanide giving $Ir(N\hat{}C)_2(RNC)(CN)$. The X-ray structures for two of the complexes show that the trans-pyridyl/cis-phenyl geometry of the parent dimer is preserved, with the ancillary ligands positioned trans to the cyclometalated phenyls. The cyano complexes all display strong blue photoluminescence in ambient, deoxygenated solutions with the first λ_{max} ranging from 441 to 458 nm, quantum yields spanning 0.60 to 0.75, and luminescent lifetimes of 12.0–21.4 μs. A lack of solvatochromism and highly structured emission indicate that the lowest energy excited state is triplet ligand centered with some admixture of singlet metal-to-ligand charge-transfer character.

Introduction

Iridium cyclometalated complexes have received considerable attention in recent years because of their favorable photochemical and photophysical properties such as good stability, high photoluminescence (PL) quantum yields, ease of spectral tuning, short triplet state lifetimes, and the ability to participate in outer sphere electron-transfer reactions.[1] Furthermore, this class of complexes has been applied to a variety of photonic applications including oxygen sensing,[2] biological labeling,[3] photosensitization,[4] and emissive materials in electrochemiluminescent[5] and organic light emitting diodes (OLEDs).[6]

Emission from iridium cyclometalates typically originates from a mixed ligand centered (LC)/metal-to-ligand charge-transfer (MLCT) state, in contrast to bi- and ter-pyridyl complexes of Ru and Os which are primarily MLCT emitters.[7] Using *fac*-Ir(ppy)$_3$ (ppy = 2-phenylpyridine) as a

* To whom correspondence should be addressed. E-mail: kenneth.dedeian@devalcol.edu. Tel.: 215-489-2462. Fax: 215-489-4960.

(1) (a) King, K. A.; Spellane, P. J.; Watts, R. J. *J. Am. Chem. Soc.* **1985**, *107*, 1431−1432. (b) Dedeian, K.; Djurovich, P. I.; Garces, F. O.; Carlson, G.; Watts, R. J. *Inorg. Chem.* **1991**, *30*, 1687−1688. (c) Lamansky, S.; Djurovich, P.; Murphy, D.; Abdel-Razzaq, F.; Kwong, R.; Tsyba, I.; Bortz, M.; Mui, B.; Bau, R.; Thompson, M. E. *Inorg. Chem.* **2001**, *40*, 1704−1711. (d) Namdas, E. B.; Ruseckas, A.; Samuel, I. D. W.; Lo, S.-C.; Burn, P. L. *J. Phys. Chem. B* **2004**, *108*, 1570−1577.

(2) (a) Vanderdonckt, E.; Camerman, B.; Hendrick, F.; Herne, R.; Vandeloise, R. *Bull. Soc. Chim. Belg.* **1994**, *103*, 207−211. (b) Amao, Y.; Ishikawa, Y.; Okura, I. *Anal. Chim. Acta* **2001**, *445*, 177−182.

(3) (a) Lo, K. K.-W.; Chung, C.-K.; Lee, T. K.-M.; Lui, L.-H.; Tsang, K. H.-K.; Zhu, N. *Inorg. Chem.* **2003**, *42*, 6886−6897. (b) Lo, K. K.-W.; Chung, C.-K.; Zhu, N. *Chem.—Eur. J.* **2003**, *9*, 475−483.

(4) (a) Gao, R.; Ho, D. G.; Hernandez, B.; Selke, M.; Murphy, D.; Djurovich, P. I.; Thompson, M. E. *J. Am. Chem. Soc.* **2002**, *124*, 14828−14829. (b) Goldsmith, J. I.; Hudson, W. R.; Lowry, M. S.; Anderson, T. H.; Bernhard, S. *J. Am. Chem. Soc.* **2005**, *127*, 7502−7510.

(5) Kapturkiewcz, A.; Angulo, G. *J. Chem. Soc., Dalton Trans.* **2003**, 3907−3913.

(6) (a) Adachi, C.; Baldo, M. A.; Forrest, S. R. *Appl. Phys. Lett.* **2000**, *77*, 904−906. (b) Wang, Y.; Herron, N.; Grushin, V. V.; LeCloux, D. D.; Petrov, V. A. *Appl. Phys. Lett.* **2001**, *79*, 449−451. (c) Ostrowski, J. C.; Robinson, M. R.; Heeger, A. J.; Bazan, G. C. *Chem. Commun.* **2002**, 784−785. (d) Markham, J. P. J.; Lo, S.-C.; Magennis, S. W.; Burn, P. L.; Samuel, I. D. W. *Appl. Phys. Lett.* **2002**, *80*, 2645−2647. (e) Holmes, R. J.; Forrest, S. R.; Tung, Y.-J.; Kwong, R. C.; Brown, J. J.; Garon, S.; Thompson, M. E. *Appl. Phys. Lett.* **2003**, *82*, 2422−2424. (f) Laskar, I. R.; Hsu, S.-F.; Chen, T.-M. *Polyhedron* **2005**, *24*, 189−200. (g) Holder, E.; Langeveld, B. M. W.; Schubert, U. S. *Adv. Mater.* **2005**, *17*, 1109−1121. (h) Kawamura, Y.; Goushi, K.; Brooks, J.; Brown, J. J.; Sasabe, H.; Adachi, C. *Appl. Phys. Lett.* **2005**, *86*, 071104.

10.1021/ic061513v CCC: $37.00
Published on Web 12/24/2006

prototypical example, we find that mixing of the π symmetry orbitals of the coordinated phenyl with the valence 5d orbitals of iridium results in a highest occupied molecular orbital (HOMO) with mixed phenyl−iridium character.[8] The lowest unoccupied molecular orbital (LUMO), on the other hand, is primarily phenylpyridine based. Exited state tuning in this class of compound has proven to be quite feasible where PL from the near-UV to deep red has been reported.[9] A common method of tuning is by modification of the cyclometalating ring system, either by the addition of substituents, expanding the size of the π system, or by introducing heteroatoms. In addition, ancillary ligands may be introduced to the metal coordination sphere. This last approach has been explored in detail recently in a study involving $Ir(tpy)_2(LL')^{0/+}$ (tpy = 2-(*p*-tolyl)pyridine) where LL′ represents one bidentate or two monodentate ligands with a range of electron withdrawing/donating properties.[10] It has been found that electron withdrawing ancillary ligands cause a blue shift in the emission and lessen the amount of MLCT mixing in the LC excited state. This occurs because of a lowering in energy of the iridium d orbitals, which participates in the HOMO, but with little change to the energy of the LUMO.

The effect of coordination by the monodentate ligands cyanide and isocyanide on the emission properties of rhodium and iridium cyclometalates has also been investigated. Room-temperature LC emission could be observed for the anion $Rh(ppy)_2(CN)_2^-$ at 460 nm ($\Phi = 0.006$) in solution.[11] Room-temperature emission is typically not observed in complexes of rhodium because of quenching by proximal, nonradiative, metal-centered states. In the iridium analogue $Ir(ppy)_2(CN)_2^-$, an exceptionally high quantum yield of near unity has been reported.[12] In addition, the emission spectrum is blue-shifted approximately 40 nm compared to that of *fac*-$Ir(ppy)_3$, a consequence of the strong electron withdrawing property of cyanide. Enhancement of the quantum yield, in both cases, has been attributed to a rise in energy of the dd states by the strong field cyanides. Isocyanide is another strong field ligand whose powerful electron withdrawing property is often exploited to stabilized low oxidation state metals.[13] Inclusion of this ligand in the cation $Ir(tpy)_2$(*t*-butyl isocyanide)$_2^+$, moves the MLCT state to rather high energy, resulting in a principally LC emitting state with $\lambda_{max} = 458$ nm.[10]

Chart 1. Cyclometalating and Isonitrile Ligands Used and the Resulting Complexes

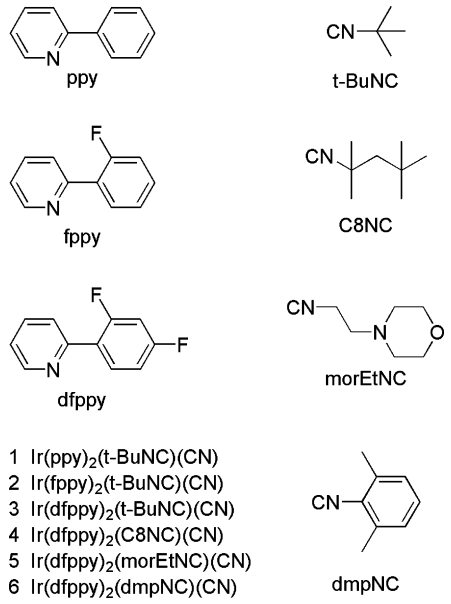

There is a continuing interest in discovering efficient, high-energy-emitting materials for a variety of optoelectronic applications. In this report, we describe the synthesis, structure, and photophysical properties of cyclometalated iridium complexes that include *both* cyanide and isocyanide ancillary ligands. The neutral species $Ir(N^C)_2(RNC)(CN)$ (Chart 1) are stable in solution and in air and are highly photoluminescent in deoxygenated solutions. The principally LC emission is well within the blue spectral region, with the first emission maxima ranging from 441 to 458 nm.

Experimental Methods

Mass spectra were measured on a Waters ZQ mass spectrometer operating in ESI+ mode. Elemental analyses were performed by Desert Analytics. ^{1}H NMR spectra were measured at the University of Maryland, College Park, Chemistry Department, on a Bruker AV-400 spectrometer and referenced to a residual protonated solvent. Absorption spectra were recorded on a Hewlett-Packard 4853 UV−vis diode array spectrometer. Emission measurements were made at room temperature using spectroscopic grade dichloromethane (Aldrich). Emission spectra were recorded on a SPEX Fluorolog spectrofluorimeter equipped with 0.22 m double monochromators and an electronically cooled Hamamatsu R928 photomultiplier tube (PMT), which has been corrected for spectral response. Quinine sulfate in 1 N H_2SO_4 ($\Phi = 0.55$) was used as the standard for quantum yield measurements. Sample quantum yields, Φ_s, were calculated from the equation $\Phi_s = \Phi_r(\eta_s^2 B_r I_s / \eta_r^2 B_s I_r)$, where Φ_r is the quantum yield of the reference, η is the refractive index of the solvents, B is the fraction of light absorbed at the excitation wavelength, and I is the integrated area under the emission spectra. Samples were bubbled with solvent saturated nitrogen in septum sealed vials for 10 min prior to recording spectra. Excitations for luminescence lifetime measurements were made by 355 nm pulses (10 ns duration) from a Coherent Infinity 40-100 Nd:YAG laser. The SPEX instrument was used for emission

(7) (a) Balzani, V.; Juris, A.; Barigelletti, F.; Campagna, S.; Belser, P.; Von Zelewsky, A. *Coord. Chem. Rev.* **1988**, *84*, 85−277. (b) Sauvage, J. P.; Collin, J. P.; Chambron, J. C.; Guillerez, S.; Coudret, C.; Balzani, V.; Barigelletti, F.; DeCola, L.; Flamigni, L. *Chem. Rev.* **1994**, *94*, 993−1019.
(8) (a) Hay, P. J. *J. Phys. Chem. A* **2002**, *106*, 1634−1641. (b) Nozaki, K. *J. Chin. Chem. Soc.* **2006**, *53*, 101−112.
(9) (a) Holmes, R. J.; Forrest, S. R.; Sajoto, T.; Tamayo, A.; Djurovich, P. I.; Thompson, M. E.; Brooks, J.; Tung, Y.-J.; D'Andrade, B. W.; Weaver, M. S.; Kwong, R. C.; Brown, J. J. *Appl. Phys. Lett.* **2005**, 243507. (b) Tsuboyama, A.; Iwawaki, H.; Furugori, M.; Mukaide, T.; Kamatani, J.; Igawa, S.; Moriyama, T.; Miura, S.; Takiguchi, T.; Okada, S.; Hoshino, M.; Ueno, K. *J. Am. Chem. Soc.* **2003**, *125*, 12971−12979.
(10) Li, J.; Djurovich, P. I.; Alleyne, B. D.; Yousufuddin, M.; Ho, N. N.; Thomas, J. C.; Peters, J. C.; Bau, R.; Thompson, M. E. *Inorg. Chem.* **2005**, *44*, 1713−1727.
(11) Kunkely, H.; Vogler, A. *Chem. Phys. Lett.* **2000**, *319*, 486−488.
(12) Nazeeruddin, M. K.; Humphry-Baker, R.; Berner, D.; Rivier, S.; Zuppiroli, L.; Graetzel, M. *J. Am. Chem. Soc.* **2003**, *125*, 8790−8797.
(13) Collman, J. P.; Hegedus, L. S.; Norton, J. R.; Finke, R. G. *Principles and Applications of Organotransition Metal Chemistry;* University Science Books: Mill Valley, CA, 1987.

Table 1. Crystallographic Data for **3** and for **6**

	3	**6**
chemical formula	$C_{28}H_{21}F_4IrN_4$	$C_{32}H_{21}F_4N_4Ir$
formula weight, amu	681.69	729.73
space group (no.)	$P2_1/n$	$P\bar{1}$
a, Å	9.8934(3)	8.2962(9)
b, Å	15.7855(4)	10.279(1)
c, Å	15.7627(4)	16.330(2)
α, deg	90	76.422(2)
β, deg	90.837(1)	83.913(2)
γ, deg	90	80.958(2)
V, Å^3	2461.4(1)	1333.3(3)
Z	4	2
T, K	193(2)	295(2)
D_{calcd}, g cm^{-3}	1.840	1.818
μ, mm^{-1}	5.480	5.065
no. collected reflections	29372	17400
no. independent reflections	5636	6047
no. observed reflections ($I > \sigma I$)	4982	5650
no. parameters	352	393
$R(F_o)$,[a] $I > 2\sigma I$	0.0210	0.0183
$R_w(F_o^2)$,[b] all data	0.0472	0.0457

[a] $R = (\sum||F_o| - |F_c||)/\sum|F_o|$. [b] $R_w = [\sum w(F_o^2 - F_c^2)^2/\sum w(F_o^2)^2]^{1/2}$.

wavelength selection and detection. The excitation beam was directed into the SPEX sample housing via a fiber optic cable. The PMT decay was monitored on a Tektronix 11402 digitizing oscilloscope, and curve fitting was performed using Origin data analysis software.

Electrochemistry. Electrochemical measurements were performed using a CH Instruments CHI660A electrochemical workstation. The electrochemical cell was located inside a faraday cage and consisted of a glassy carbon working electrode, platinum wire counter electrode, and Ag/AgCl reference electrode that was isolated by a salt bridge. The electrolyte solution consisted of 0.1 M N(*n*-Bu)$_4$PF$_6$ (TBAH) in anhydrous, nitrogen saturated dimethylformamide (DMF, Aldrich). Potentials were determined using differential pulse voltammetry and are referenced to the ferrocenium/ferrocene redox couple, whereas electrochemical reversibility was ascertained by cyclic voltammetry.

X-ray Crystallography. Crystals of **3** and **6** were grown from slowly evaporating solutions of toluene/methanol and dichloromethane/acetonitrile, respectively. X-ray diffraction data were collected on a Bruker SMART 1000 CCD diffractometer (graphite monochromator, Mo Kα radiation, $\lambda = 0.717\ 03$ Å). The final cell parameters were obtained from the least-squares refinement of spots with $I > 10\sigma I$ during the intensity integration using the SAINT Plus program. A near full sphere of the crystal data was collected up to a resolution of 0.76 Å ($2\theta_{max} = 55°$) providing at least 99% coverage of independent reflections. All calculations for the structure determination were carried out using the SHELXTL package (version 5.1).[14] Absorption correction was applied by using SADABS.[15] Crystal structures were solved using direct methods. Positions of H atoms were constrained to be riding along with the attached carbons; however, their isotropic displacement parameters were refined independently as an additional proof of their correctness. A summary of the refinement details and resulting factors is given in Table 1.

Density Functional Theory Calculations. DFT calculations were performed using Spartan '04 software (Wavefunction) using the B3LYP hybrid functional and the 6-31G* basis set. The HOMO and LUMO orbitals were obtained for the minimized singlet ground state geometries.

Synthesis. Cyclometalated dichloro-bridged iridium dimers were reacted with isocyanide ligands to give intermediate products $\mathbf{1}_{Cl}$−$\mathbf{6}_{Cl}$. In turn, these were converted to the cyano species **1**−**6**. Detailed procedures for synthesizing complexes $\mathbf{6}_{Cl}$ and **6** are given below. All other complexes were made and purified in a similar manner. 2-Phenylpyridine and the isocyanide ligands were purchased (Aldrich) whereas 2-(2-fluorophenyl)pyridine, 2-(2,4-difluorophenyl)pyridine, and the dichloro-bridged dimers were made following literature methods.[16]

Ir(dfppy)$_2$(dmpNC)(Cl) ($\mathbf{6}_{Cl}$). 2,6-Dimethylphenyl isocyanide (0.535 g, 4.08 mmol) was added to a stirring suspension of [Ir(dfppy)$_2$Cl]$_2$ (2.36 g, 3.88 mmol) in dichloromethane (50 mL). After 1 h, the now clear solution was poured onto a silica gel column and eluted with CH_2Cl_2 in order to remove the less polar impurities. The mobile phase was then switched to 95:5 CH_2Cl_2:MeOH in order to elute the product. Evaporation under reduced pressure led to the precipitation of a bright yellow solid, which was filtered off, washed with MeOH, and air-dried. Yield: 2.31 g, 80%. MS *m*/*z*: 704.0 (M − Cl). ^{1}H NMR (400 MHz, $CDCl_3$, ppm): 9.99 (dd, 1H, J = 5.8, 1.5 Hz), 9.23 (dd, 1H, J = 5.8, 1.5 Hz), 8.35 (d, 1H, J = 8.0 Hz), 8.30 (d, 1H, J = 8.5 Hz), 7.90 (m, 2H), 7.33 (ddd, 1H, J = 7.3, 5.8, 1.3 Hz), 7.20 (ddd, 1H, J = 7.3, 6.0, 1.5 Hz), 7.15 (dd, 1H, J = 8.0, 7.0 Hz), 7.04 (d, 2H, J = 7.5 Hz), 6.41 (m, 2H), 5.86 (dd, 1H, J = 8.5, 2.3 Hz), 5.59 (dd, 1H, J = 8.3, 2.5 Hz), 2.16 (s, 6H).

Ir(dfppy)$_2$(dmpNC)(CN) (6). $\mathbf{6}_{Cl}$ (2.00 g, 2.70 mmol), $AgCF_3CO_2$ (800 mg, 3.62 mmol), and MeOH (200 mL) were heated to ∼50 °C with stirring. After 0.5 h the AgCl precipitate was removed by filtration. To the clear, light yellow filtrate was added NaCN (250 mg, 5.10 mmol) dissolved in 40 mL of water. The mixture was heated to reflux for 0.5 h and was then concentrated to ∼100 mL by evaporation. The resulting pale yellow product was collected by filtration and washed with MeOH. The product was dissolved in CH_2Cl_2 and was chromatographed as per $\mathbf{6}_{Cl}$ above. Yield: 1.10 g, 56%. MS *m*/*z*: 731.0 (M + H). Anal. Calcd for $IrC_{32}H_{21}N_4F_4$: C, 52.67; H, 2.90; N, 7.68. Found: C, 52.37; H, 2.92; N, 7.63. ^{1}H NMR (400 MHz, CD_2Cl_2, ppm): 9.77 (ddd, 1H, J = 5.8, 1.8, 0.8 Hz), 9.18 (ddd, 1H, J = 5.8, 1.5, 0.8 Hz), 8.35 (m, 2H), 7.96 (m, 2H), 7.33 (ddd, 1H, J = 7.5, 6.0, 1.5 Hz), 7.24 (ddd, 1H, J = 7.3, 6.0, 1.5 Hz), 7.18 (dd, 1H, J = 8.3, 6.8 Hz), 7.08 (d, 2H, J = 7.8 Hz), 6.47 (m, 2H), 5.83 (dd, 1H, J = 8.0, 2.3 Hz), 5.71 (dd, 1H, J = 8.5, 2.5 Hz), 2.16 (s, 6H).

Ir(ppy)$_2$(*t*-BuNC)(Cl) ($\mathbf{1}_{Cl}$). Yield 82%. MS *m*/*z*: 584.0 (M − Cl). ^{1}H NMR (400 MHz, $CDCl_3$, ppm): 9.92 (ddd, 1H, J = 6.0, 1.5, 0.8 Hz), 9.08 (ddd, 1H, J = 5.8, 1.5, 0.8 Hz), 7.87 (m, 2H), 7.80 (m, 2H), 7.56 (m, 2H), 7.24 (ddd, 1H, J = 7.0, 5.5, 1.5 Hz), 7.13 (ddd, 1H, J = 7.5, 5.8, 1.5 Hz), 6.85 (m, 2H), 6.79 (ddd, 1H, J = 7.3, 7.3, 1.5 Hz), 6.74 (ddd, 1H, J = 7.5, 7.5, 1.5 Hz), 6.35 (dd, 1H, J = 7.8, 1.3 Hz), 6.11 (dd, 1H, J = 7.3, 1.3 Hz), 1.33 (s, 9H).

Ir(ppy)$_2$(*t*-BuNC)(CN) (1). Yield 29%. MS *m*/z: 611.0 (M + H). Anal. Calcd for $IrC_{28}H_{25}N_4$: C, 55.15; H, 4.13; N, 9.19. Found: C, 54.95; H, 4.09; N, 9.13. ^{1}H NMR (400 MHz, 95:5 CD_2Cl_2/CD_3OD, ppm): 9.58 (ddd, 1H, J = 5.8, 1.4, 0.8 Hz), 9.08 (ddd, 1H, J = 6.0, 1.5, 0.8 Hz), 7.96 (m, 2H), 7.89 (m, 2H), 7.65 (m, 2H), 7.28 (ddd, 1H, J = 7.0, 5.9, 1.9 Hz), 7.21 (ddd, 1H, J = 7.3, 5.9, 1.6 Hz), 6.95 (ddd, 1H, J = 7.4, 3.7, 1.3 Hz), 6.93 (ddd, 1H,

(14) Sheldrick, G. M. *SHELXTL*, version 5.1; Bruker Analytical X-ray System, Inc.: Madison, WI, 1997.
(15) Sheldrick, G. M. *SADABS;* University of Göttingen: Göttingen, Germany, 1996.
(16) (a) Negishi, E.; Luo, F.-T.; Frisbee, R.; Matsushita, H. *Heterocycles* **1982**, *18*, 117−122. (b) Littke, A. F.; Dai, C.; Fu, G. C. *J. Am. Chem. Soc.* **2000**, *122*, 4020−4028. (c) Sprouse, S.; King, K. A.; Spellane, P. J.; Watts, R. J. *J. Am. Chem. Soc.* **1984**, *106*, 6647−6653.

J = 7.7, 3.8, 1.3 Hz), 6.83 (m, 2H), 6.26 (dd, 1H, J = 7.5, 1.1 Hz), 6.18 (dd, 1H, J = 7.6, 1.1 Hz), 1.34 (s, 9H).

Ir(fppy)$_2$(*t*-BuNC)(Cl) (2_{Cl}). Yield 89%. MS *m*/*z*: 620.0 (M − Cl). ^{1}H NMR (400 MHz, $CDCl_3$, ppm): 9.97 (dd, 1H, J = 6.0, 1.6 Hz), 9.11 (dd, 1H, J = 5.8, 1.5 Hz), 8.37 (dd, 1H, J = 8.3, 3.0 Hz), 8.33 (d, 1H, J = 8.5 Hz), 7.85 (m, 2H), 7.28 (ddd, 1H, J = 7.3, 5.8, 1.3 Hz), 7.16 (ddd, 1H, J = 7.5, 6.0, 1.5 Hz), 6.76 (m, 2H), 6.56 (m, 2H), 6.09 (dd, 1H, J = 7.5, 0.7 Hz), 5.86 (d, 1H, J = 7.3 Hz), 1.35 (s, 9H).

Ir(fppy)$_2$(*t*-BuNC)(CN) (2). Yield 62%. MS *m*/*z*: 647.0 (M + H). Anal. Calcd for $IrC_{28}H_{23}N_4F_2$: C, 52.08; H, 3.59; N, 8.68. Found: C, 51.81; H, 3.75; N, 8.42. ^{1}H NMR (400 MHz, CD_2Cl_2, ppm): 9.73 (ddd, 1H, J = 5.9, 1.8, 0.6 Hz), 9.05 (ddd, 1H, J = 5.8, 1.5, 0.7 Hz), 8.38 (m, 2H), 7.92 (m, 2H), 7.29 (ddd, 1H, J = 7.3, 5.8, 1.4 Hz), 7.22 (ddd, 1H, J = 7.4, 5.8, 1.4 Hz), 6.82 (m, 2H), 6.63 (m, 2H), 6.04 (d, 1H, J = 7.3 Hz), 5.95 (d, 1H, J = 7.3 Hz), 1.35 (s, 9H).

Ir(dfppy)$_2$(*t*-BuNC)(Cl) (3_{Cl}). Yield 88%. MS *m*/*z*: 656.0 (M − Cl). ^{1}H NMR (400 MHz, $CDCl_3$, ppm): 9.89 (dd, 1H, J = 6.0, 1.6 Hz), 9.03 (dd, 1H, J = 5.8, 1.5 Hz), 8.31 (d, 1H, J = 8.3 Hz), 8.27 (d, 1H, J = 8.3 Hz), 7.87 (m, 2H), 7.30 (ddd, 1H, J = 7.3, 6.0, 1.3 Hz), 7.18 (ddd, 1H, J = 7.3, 5.8, 1.3 Hz), 6.38 (m, 2H), 5.77 (dd, 1H, J = 8.7, 2.3 Hz), 5.52 (dd, 1H, J = 8.3, 2.3 Hz), 1.38 (s, 9H).

Ir(dfppy)$_2$(*t*-BuNC)(CN) (3). Yield 52%. MS *m*/*z*: 683.0 (M + H). Anal. Calcd for $IrC_{28}H_{21}N_4F_4$: C, 49.33; H, 3.11; N, 8.22. Found: C, 49.12; H, 3.23; N, 7.89. ^{1}H NMR (400 MHz, 95:5 CD_2Cl_2/CD_3OD, ppm): 9.59 (ddd, 1H, J = 5.8, 1.6, 0.8 Hz), 8.98 (ddd, 1H, J = 5.9, 1.6, 0.7 Hz), 8.33 (m, 2H), 7.96 (m, 2H), 7.32 (ddd, 1H, J = 7.4, 5.8, 1.4 Hz), 7.25 (ddd, 1H, J = 7.3, 5.8, 1.4 Hz), 6.44 (m, 2H), 5.73 (dd, 1H, J = 8.0, 2.4 Hz), 5.63 (dd, 1H, J = 8.3, 2.4 Hz), 1.37 (s, 9H).

Ir(dfppy)$_2$(C8NC)(Cl) (4_{Cl}). Yield 72%. MS *m*/*z*: 712.1 (M − Cl). ^{1}H NMR (400 MHz, $CDCl_3$, ppm): 9.91 (dd, 1H, J = 6.0, 1.8 Hz), 9.03 (dd, 1H, J = 5.8, 1.7 Hz), 8.31 (d, 1H, J = 8.3 Hz), 8.25 (d, 1H, J = 8.3 Hz), 7.87 (m, 2H), 7.29 (ddd, 1H, J = 7.3, 5.8, 1.3 Hz), 7.17 (ddd, 1H, J = 7.3, 6.0, 1.3 Hz), 6.37 (m, 2H), 5.77 (dd, 1H, J = 8.5, 2.5 Hz), 5.54 (dd, 1H, J = 8.3, 2.3 Hz), 1.45 (s, broad, 8H), 0.73 (s, 9H).

Ir(dfppy)$_2$(C8NC)(CN) (4). Yield 22%. MS *m*/*z*: 739.1 (M + H). Anal. Calcd for $IrC_{32}H_{29}N_4F_4$: C, 52.09; H, 3.96; N, 7.59. Found: C, 51.78; H, 4.03; N, 7.31. ^{1}H NMR (400 MHz, CD_2Cl_2, ppm): 9.68 (ddd, 1H, J = 5.9, 1.8, 0.8 Hz), 8.98 (ddd, 1H, J = 5.9, 1.6, 0.8 Hz), 8.32 (m, 2H), 7.93 (m, 2H), 7.29 (ddd, 1H, J = 7.4, 5.8, 1.4 Hz), 7.23 (ddd, 1H, J = 7.4, 5.9, 1.5 Hz), 6.43 (m, 2H), 5.74 (dd, 1H, J = 8.0, 2.4 Hz), 5.66 (dd, 1H, J = 8.3, 2.4 Hz), 1.49 (s, 1H), 1.47 (s, 4H), 1.44 (s, 3H), 0.74 (s, 9H).

Ir(dfppy)$_2$(morEtNC)(Cl) (5_{Cl}). Yield 82%. MS *m*/*z*: 713.1 (M − Cl). ^{1}H NMR (400 MHz, $CDCl_3$, ppm): 9.89 (dd, 1H, J = 6.0, 1.8 Hz), 9.21 (dd, 1H, J = 5.8, 1.5 Hz), 8.32 (dd, 1H, J = 8.3, 2.5 Hz), 8.28 (d, 1H, J = 8.3 Hz), 7.89 (m, 2H), 7.31 (ddd, 1H, J = 7.5, 6.0, 1.5 Hz), 7.19 (ddd, 1H, J = 7.3, 5.8, 1.3 Hz), 6.38 (m, 2H), 5.79 (dd, 1H, J = 8.5, 2.3 Hz), 5.48 (dd, 1H, J = 8.3, 2.3 Hz), 3.70 (m, 2H), 3.60 (m, 4H), 2.60 (m, 2H), 2.38 (m, 4H).

Ir(dfppy)$_2$(morEtNC)(CN) (5). Yield 36%. MS *m*/*z*: 740.0 (M + H). Anal. Calcd for $IrC_{30}H_{24}N_5F_4O$: C, 48.77; H, 3.27; N, 9.48. Found: C, 48.67; H, 3.40; N, 9.47. ^{1}H NMR (400 MHz, CD_2Cl_2), ppm: 9.68 (ddd, 1H, J = 6.0, 1.8, 0.8 Hz), 9.17 (ddd, 1H, J = 5.8, 1.8, 0.8 Hz), 8.33 (m, 2H), 7.95 (m, 2H), 7.31 (ddd, 1H, J = 7.3, 5.8, 1.5 Hz), 7.24 (ddd, 1H, J = 7.0, 5.8, 1.3 Hz), 6.44 (m, 2H), 5.76 (dd, 1H, J = 8.0, 2.5 Hz), 5.60 (dd, 1H, J = 8.3, 2.5 Hz), 3.73 (m, 2H), 3.55 (m, 4H), 2.57 (m, 2H), 2.34 (m, 4H).

Scheme 1. Reaction Sequence to Cyano/Isocyanide Complexes[a]

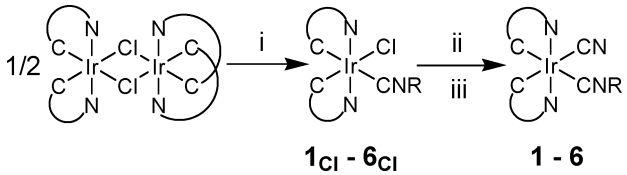

[a] (i) Isocyanide ligand, dichloromethane. (ii) $AgCF_3CO_2$, MeOH. (iii) NaCN, H_2O.

Results and Discussion

Synthesis and Structure. Cyclometalated dichloro-bridged iridium dimers are readily cleaved by isocyanide ligands to give monomers of the type Ir(N^C)$_2$(RNC)(Cl), $\mathbf{1}_{Cl}$−$\mathbf{6}_{Cl}$, in high yields, Scheme 1. Mono- and bidentate ligands are known to displace chloride and enter into the coordination sphere while preserving the chelate ligands trans-N,N cis-C,C disposition about the iridium center.[17] In the second step, the chloride is extracted by silver salts and is replaced by cyanide, giving **1**−**6** in moderate yields. Precipitation of the final product begins soon after the addition of aqueous sodium cyanide. To chromatograph, the chloro and cyano products were loaded on a silica gel column and washed with dichloromethane to remove the less polar impurities. To move the product off of the column, it is necessary to switch to a mobile phase containing alcohol. Although not soluble in neat methanol, the cyano complexes' solubility is greatly increased by the addition of a small amount of methanol to an otherwise poor solvent (such as toluene). Methanol likely aids dissolution by hydrogen bonding with the polar cyano ligand of the otherwise hydrophobic metal complex. Furthermore, in the mass spectra of **1**−**6**, the parent ion is the protonated form of the molecule. Protonation is likely to occur at the N-terminus of CN. Protonation does not occur for $\mathbf{1}_{Cl}$−$\mathbf{6}_{Cl}$; rather, loss of chloride is observed.

The ^{1}NMR spectrum of **1** integrates for 16 aromatic protons at δ = 9.6 to 6.1. The phenylpyridines for each of the 12 complexes are magnetically inequivalent because of a lack of molecular symmetry. In the spectra of **6**, in addition to the 12 aromatic protons from dfppy, there are also resonances at δ = 7.18 and 7.08 arising from the aromatic protons of dimethylphenyl isocyanide. The benzylic protons are observed at δ = 2.16.

The X-ray crystal structures of **3** and **6** are shown in Figure 1. Both complexes assume the same geometry about the metal center with mutually trans pyridyls and cis phenyls and with the cyanide and isocyanide ligands positioned trans to the phenyl−Ir bonds. Hence, the difluorophenylpyridines of the dimer precursor did not undergo isomerization in the multistep synthesis. Select bond lengths and bond angles are given in Table 2. Not surprisingly, corresponding metric parameters between the two complexes are very similar; the largest bond length difference occurs for Ir−$C_{isocyanide}$ (δ = 0.03 Å). The isocyanides form the shortest bonds to iridium, whereas the bond to cyanide is, on average, 0.06 Å longer.

(17) King, K. A.; Finlayson, M. F.; Spellane, P. J.; Watts, R. J. *Sci. Pap. Inst. Phys. Chem. Res. (Jpn.)* **1984**, *78*, 97−106.

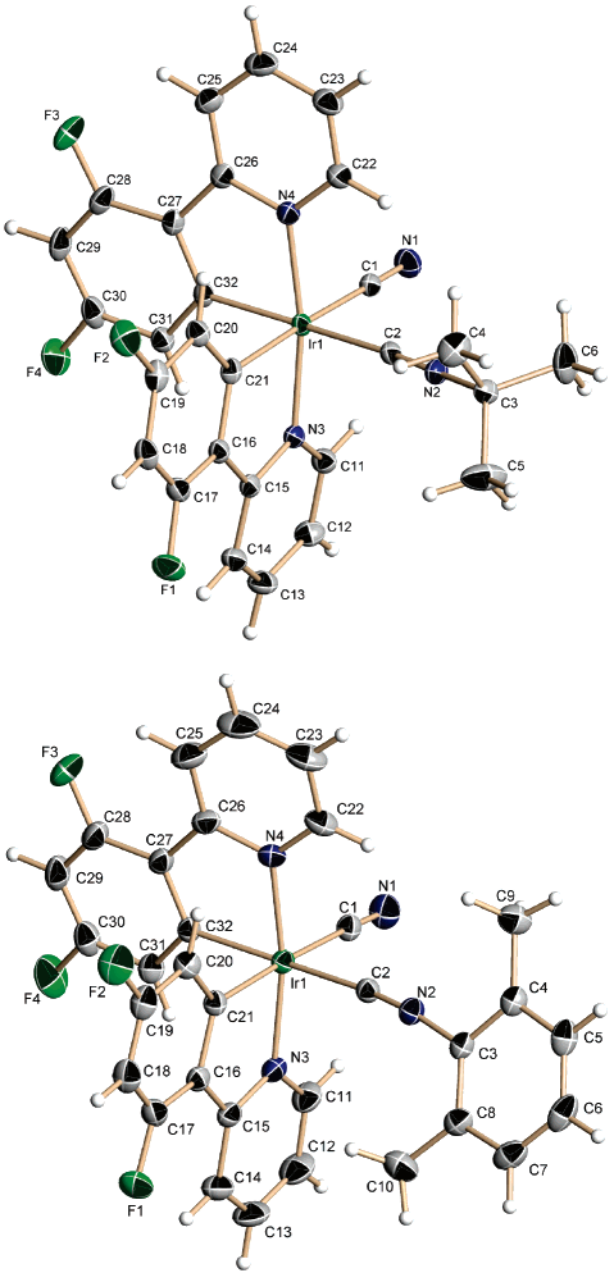

Figure 1. Views of molecules **3** (top) and **6** (bottom) showing the numbering scheme employed. Anisotropic atomic displacement ellipsoids for the non-hydrogen atoms are shown at the 30% probability level. Hydrogen atoms are displayed with an arbitrarily small radius.

The Ir−C_{phenyl} bonds opposite to cyanide are approximately 0.015 Å longer than those opposite to isocyanides, demonstrating that cyanide exerts a slightly stronger trans influence than isocyanide. Corresponding bond angles of the two complexes are also very similar. The Ir−C−N bond angles involving cyanide are nearly linear at 178°, whereas the Ir−C−N angle involving isocyanide is slightly bent at around 172°.

DFT Calculations. DFT calculations were performed on complexes **3** and **6** at the B3LYP level using unconstrained geometry. The metric parameters obtained are in close agreement to the crystallographic values. In the case of **3**, the calculated iridium−donor atom bond lengths are Ir−$N_{average}$ (2.085 Å), Ir−$C_{phenyl,trans\ CN}$ (2.07 Å), Ir−$C_{phenyl,trans\ RNC}$ (2.06 Å), Ir−C_{CN} (2.08 Å), and Ir−C_{RNC} (2.01 Å). The contour plots of the valence orbitals are very similar for each complex, and the plots of **6** are shown in Figure 2. The HOMO is comprised mostly of π-phenyl, d-iridium, and π-cyanide orbitals. The LUMO is localized on one of the dfppy ligands, whereas the LUMO + 1 is located on the other dfppy at 50−80 mV higher energy. It is not until LUMO + 4, which is 1.7 eV above the LUMO, does the contour plot for **3** reveal significant π-isocyanide character. Therefore, for complexes **1**−**5**, with alkyl groups bonded to the N of isocyanide, it is not expected that the isocyanide ligands play any direct role in the lower energy electronic transitions. However for **6**, LUMO + 2 is primarily dmpNC in character, and it is only 260 mV above the LUMO. It may then be expected that charge-transfer transitions involving dmpNC could appear at energies only somewhat higher than those involving dfppy. The absorption data (vide infra) show evidence for this.

Table 2. Selected Bond Lengths (Å) and Angles (deg) for **3** and for **6**

	3	**6**
Ir1−C1	2.064(3)	2.074(3)
Ir1−C2	2.020(3)	1.993(3)
Ir1−C21	2.056(3)	2.065(3)
Ir1−C32	2.038(3)	2.052(2)
Ir1−N3	2.056(2)	2.058(2)
Ir1−N4	2.056(3)	2.048(2)
C1−N1	1.148(4)	1.135(4)
C2−N2	1.150(4)	1.153(3)
C1−Ir1−C21	175.91(12)	175.40(10)
C2−Ir1−C32	173.09(12)	173.78(9)
N3−Ir1−N4	170.03(10)	169.62(9)
C1−Ir1−C2	94.63(12)	94.48(10)
N1−C1−Ir1	178.8(3)	177.4(3)
N2−C2−Ir1	172.3(3)	172.4(2)
C2−N2−C3	172.3(3)	172.8(3)
N3−C15−C16−C21	−7.1(4)	−2.8(3)
C14−C15−C16−C17	−10.7(5)	−4.1(5)
N4−C26−C27−C32	4.1(4)	−4.0(3)
C25−C26−C27−C28	5.1(5)	−6.5(5)
∠(N3···C15)−(C16···C21)[a]	11.7(2)	3.7(2)
∠(N4···C26)−(C27···C32)[a]	6.8(2)	8.5(2)

[a] Dihedral angles between adjacent rings.

Electrochemistry. Redox potentials for **1**−**6** are given in Table 3. The observable oxidation processes of **1**, **2**, and **5** were irreversible, whereas the oxidation of **3**, **4**, and **6** lies outside the DMF solvent window. The oxidation for **5** is assigned to the morpholine moiety since there is no oxidation observed at this potential for the other dfppy complexes. In contrast, complexes of the type Ir(N^C)$_3$ and Ir(N^C)$_2$(acac) (acac = 2,4-pentanedionato) typically undergo *reversible* phenyl−metal oxidation processes, and the oxidation of $TBA^+Ir(ppy)_2(CN)_2^-$ is reported as quasi-reversible. The isocyanide ligand may therefore be responsible for the observed electrochemical irreversibility. There is an approximately 500 mV anodic shift in the oxidation potential of **1** as compared to Ir(ppy)$_3$, demonstrating the large electron withdrawing property of the ancillary ligand pair.

Multiple, irreversible reduction processes were observed for all complexes in the cathodic scan (only the first potential is reported). However, in the cases of **2**, **5**, and **6**, the first reduction becomes reversible or quasi-reversible if the sweep

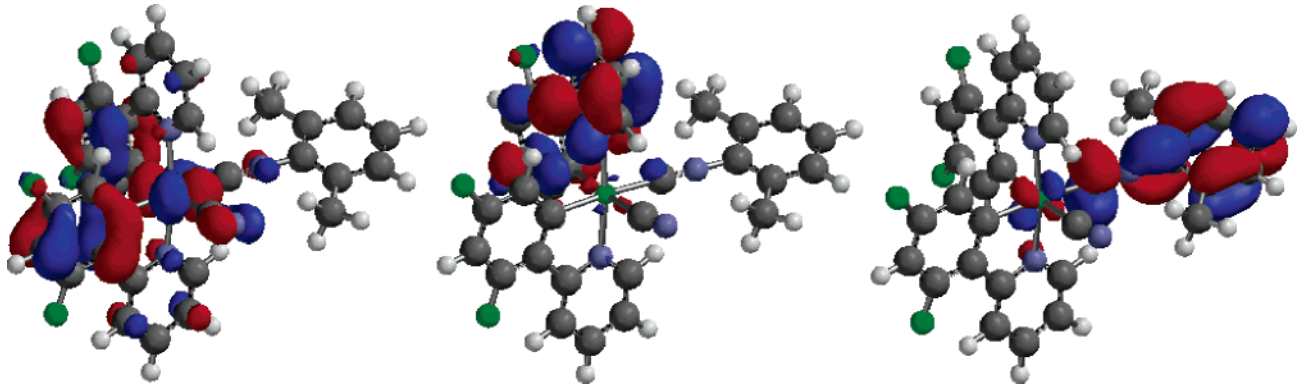

Figure 2. Contour plots for complex **6**. HOMO (left), LUMO (center), and LUMO + 2 (right).

Table 3. Photophysical and Electrochemical Data for Ir(N^C)$_2$(RCN)(CN) Complexes[a]

compound	absorption features, nm (ϵ, 10^3 cm^{-1} M^{-1})	λ_{max}, nm[b]	τ, μs	Φ	k_r, 10^4 s^{-1}	k_{nr}, 10^4 s^{-1}	E_{ox} (V)	E_{red} (V)
1	247 (35.9), 261 (32.9), 361 (6.6), 423 (0.13), 453 (0.05)	458, 490	14.0	0.67	4.8	2.4	0.84	−2.57
2	241 (39.8), 301 (17.9), 311 (17.2), 357 (5.6), 416 (0.14), 445 (0.06)	450, 480	12.0	0.70	5.8	2.5	1.06	−2.40[c]
3	242 (39.7), 297 (15.6), 308 (15.6), 348 sh (6.4), 409 (0.12), 437 (0.05)	442, 472	15.8	0.60	3.8	2.5	*d*	−2.35
4	242 (41.1), 298 (15.4), 309 (15.8), 347 sh (6.5), 409 (0.10), 437 (0.04)	442, 471	18.0	0.71	3.9	1.6	*d*	−2.37
5	242 (40.6), 298 (15.0), 308 (15.7), 347 sh (6.5), 409 (0.09), 437 (0.04)	442, 471	21.4	0.61	2.9	1.8	0.85	−2.38[c]
6	243 (49.1), 257 sh (46.2), 307 (18.5), 345 sh (6.5), 409 (0.07), 436 (0.03)	441, 471	19.2	0.75	3.9	1.3	*d*	−2.33[c]

[a] Room-temperature spectroscopic and electrochemical measurements were made in dichloromethane and DMF solvent, respectively. Electrochemical potentials are irreversible unless otherwise noted and are relative to the Fc^+/Fc couple. [b] First two highest energy peaks. [c] Reversible. [d] Oxidation outside solvent window.

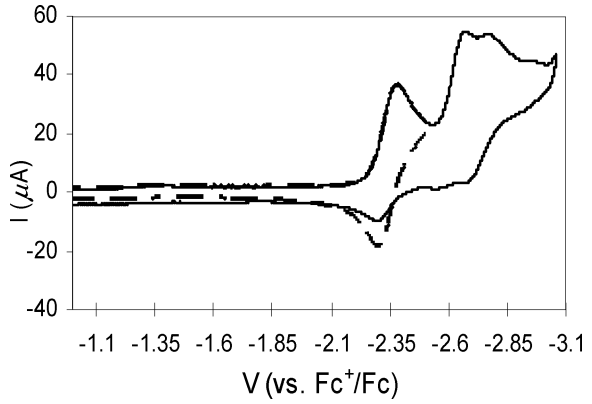

Figure 3. Cyclic voltammogram of Ir(dfppy)$_2$(dmpNC)(CN) in 0.1 M (n-Bu)$_4$N(PF$_6$) anhydrous DMF solution.

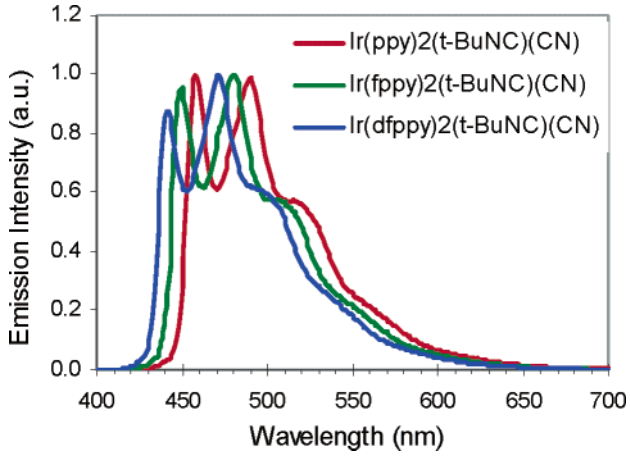

Figure 4. Room-temperature emission spectra of **1**, Ir(ppy)$_2$(*t*-BuNC)(CN); **2**, Ir(fppy)$_2$(*t*-BuNC)(CN); and **3**, Ir(dfppy)$_2$(*t*-BuNC)(CN) in dichloromethane.

is reversed immediately after the process, Figure 3. This first reduction is assigned to phenylpyridine in accordance to DFT calculation results. Although it may be possible that dmpNC in **6** can be reduced under our experimental conditions, the irreversibility of the reduction past the first wave makes that assignment impossible. It is interesting to note that the reduction of **1** is within the narrow range of potentials reported (−2.56 to −2.68 V) for related neutral Ir(tpy)$_2$(LL′) complexes.[10] In that report, it was observed that the identity of the ancillary ligand exerted only a modest effect on the reduction potential, and this seems to be true also for the cyano/isocyanide ligand pair.

Electronic Spectroscopy. The emission spectra for **1**, **2**, and **3** and the absorption and emission spectra of **6** are shown in Figures 4 and 5, respectively. A summary of the spectroscopic data is given in Table 3. All measurements were made in ambient-temperature dichloromethane solutions. Since the phosphorescence is highly quenched by oxygen, all emission measurements were made in nitrogen-flushed solutions. The absorption spectra of **1**, **2**, and **3** are provided as Supporting Information, whereas the absorption and emission spectra of **4** and **5** are nearly identical to those of **3**.

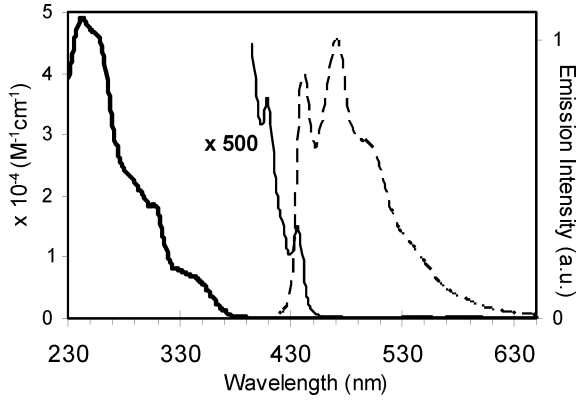

Figure 5. Absorption spectra (heavy solid), expanded absorption spectra (solid), and room-temperature emission spectra (dashed) of **6** Ir(dfppy)$_2$(dmpNC)(CN). Measured in dichloromethane.

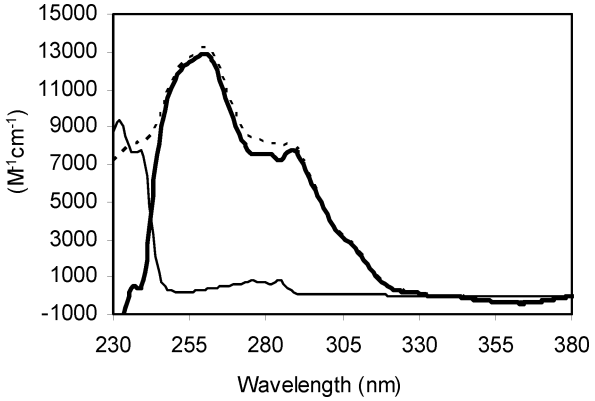

Figure 6. Differential absorption spectra of **6** minus **5** (dashed), absorption spectra of dmpNC (solid), and differential absorption spectra less the absorption of dmpNC (heavy solid).

For all complexes, the higher energy absorption peaks, ranging from 230−330 nm, are assigned to spin allowed $\pi-\pi^*$ transitions of the cyclometalating ligands. LC absorption from the dmpNC ligand of **6** also occurs in this region. Overlapping these bands and extending toward the visible are additional features, spanning 300 to 400 nm. The positions of these bands are weakly effected by solvent polarity. For example, the peak at 308 nm for **3** (measured in dichloromethane) shifts to 305 nm in MeCN and to 311 nm in toluene. Such bands are typical for cyclometalated complexes of iridium and are assigned to spin allowed Ir → phenylpyridine MLCT transitions. Common to all complexes is a weak but well-resolved peak from 436−453 nm with an extinction coefficient of 60 or less. The position of this band is invariant to solvent polarity and overlaps with the complexes' emission spectrum. Such peaks have been observed previously for $[Rh(ppy)_2Cl]_2$[16c] and for Ir(N^C)$_2$(LL′)[10] complexes with strong electron withdrawing ancillary ligands and have been interpreted as arising from a spin forbidden, ligand-centered transition with some singlet MLCT mixing, facilitated by spin−orbit coupling.

In the case of **6**, there appears to be additional strong UV absorption that is not present in the other dfppy complexes and is at lower energy than the LC absorption of free dmpNC. As noted earlier in the DFT calculations section, Ir → isocyanide charge-transfer transitions may be present in **6** at significantly lower energy than for the other complexes. Among the dfppy complexes, it is expected that the LC_{dfppy} and $MLCT_{dfppy}$ band positions and intensities will be similar; therefore, the difference in the absorption spectra of dfppy complexes **3**, **4**, or **5** and that of **6** should expose new absorption features associated with the dmpNC ligand. For example, by subtracting the absorption spectra of **5** from **6** and also subtracting the absorption contribution of the free dmpNC ligand (morEtNC absorption is negligible in this region), a differential absorption spectrum is obtained that reveals strong absorption from 240 to 320 nm, Figure 6. The differential absorption spectrum approximates the shape and position of the Ir → dmpNC charge-transfer band and shows that this transition occurs several hundred millivolts higher in energy than does the Ir → dfppy charge-transfer transition. The spectroscopic data, however, show no influence of this higher energy state on the emission properties of **6**.

The complexes **1**−**6** are all highly photoluminescent in de-oxygenated solutions, and their spectra are highly structured. Across the *t*-butyl isocyanide series, there is an 8 nm hypsochromic shift in the emission spectra for each fluorine substituent introduced to phenylpyridine. Fluorination in these ring positions is known to blue-shift the emission in cyclometalated Ir[18] and Pt[19] complexes. However, the emission spectra for all of the dfppy complexes are nearly identical to each other, demonstrating that the R group of isocyanide plays little role in modifying the electron density on iridium. The luminescent lifetimes are consistent with short-lived, predominately ^{3}LC states. The highly resolved emission structure and lack of solvatochromism also confirm the LC character of emission.

The emission energies for **1**−**6** are among the highest displayed for phenylpyridine-based complexes of iridium, Table 3. Considerable efforts are being made lately to shift the emission spectra of neutral heavy metal complexes from the green to the blue spectral region, primarily for their potential to serve as phosphors in full color or white OLEDs. Homoleptic tris complexes of iridium with substituted phenylpyridines, such as 2,4-difluorophenylpyridine,[20] 2,4-difluorophenyl-4-methoxypyridine,[21] and 2,4-difluorophenyl-10,10-dimethyl-4-aza-tricycloundeca-2,4,6-triene,[22] are highly luminescent (Φ_{PL} = 0.72−0.95) with emission maxima ranging from 469 to 475 nm. Additional blue-shifting has been reported for Ir(dfppy)$_2$(LL) where LL is picolinate,[23]

(18) Grushin, V. V.; Herron, N.; LeCloux, D. D.; Marshall, W. J.; Petrov, V. A.; Wang, Y. *Chem. Commun.* **2001**, 1494−1495.
(19) Brooks, J.; Babayan, Y.; Lamansky, S.; Djurovich, P. I.; Tsyba, I.; Bau, R.; Thompson, M. E. *Inorg. Chem.* **2002**, *41*, 3055−3066.
(20) (a) Tamayo, A. B.; Alleyne, B. D.; Djurovich, P. I.; Lamansky, S.; Tsyba, I.; Ho, N. N.; Bau, R.; Thompson, M. E. *J. Am. Chem. Soc.* **2003**, *125*, 7377−7387. (b) Dedeian, K.; Shi, J.; Shepherd, N.; Forsythe, E.; Morton, D. C. *Inorg. Chem.* **2005**, *44*, 4445−4447.
(21) Laskar, I.; Hsu, S.-F.; Chen, T.-M. *Polyhedron* **2005**, *24*, 189−200.
(22) Chew, S.; Lee, C. S.; Lee, S.-T.; Wang, P.; He, J.; Li, W.; Pan, J.; Zhang, X.; Kwong, H. *Appl. Phys. Lett.* **2006**, *88*, 093510.
(23) Holmes, R. J.; Forrest, S. R.; Tung, Y.-J.; Kwong, R. C.; Brown, J. J.; Garon, S.; Thompson, M. E. *Appl. Phys. Lett.* **2003**, *82*, 2422−2424.

substituted 5-(pyridin-2-yl)-1,2,4-triazolate,[24] 5-(pyridine-2-yl)-tetrazolate,[25] and tetrakis(1-pyrazolyl)borate,[10] where λ_{max} of the latter is at 456 nm. However, the first emission maxima of the mixed cyano−isocyanide complexes **3**−**6** are blue-shifted approximately 15 nm further still, while maintaining very high quantum efficiencies. Most recently, iridium complexes of N-heterocyclic carbenes have been reported[26] as novel UV emitting materials for OLEDs, but these species, so far, display only low to moderate PL quantum yields.

The emission spectra of the chloro precursor complexes, $\mathbf{1}_{Cl}$−$\mathbf{6}_{Cl}$, are red-shifted by 11 to 16 nm relative to spectra of their cyano analogues, and their emission intensities are much weaker. For example, the first emission maximum for $\mathbf{6}_{Cl}$ is 452 nm and $\Phi_{PL} = 0.19$. The HOMOs in the chloro and cyano complexes are primarily a mixture of π-phenyl, d-iridium, and π-Cl/CN orbitals. Relative to chloride, the pseudo-halogen cyanide lowers the energy of the HOMO resulting in a larger HOMO−LUMO gap and a higher emission energy. At the same time, the larger ligand field-splitting parameter of cyanide shifts the dd states of iridium well above that of the emitting LC state, resulting in an increase in the PL quantum yield.

Interesting trends are observed by comparing the spectroscopic properties of the previously reported anion[12] $Ir(ppy)_2(CN)_2^-$ and cation[10] $Ir(tpy)_2(t\text{-BuNC})_2^+$ to those of neutral $Ir(ppy)_2(CN)(t\text{-BuNC})$, **1**. These trends provide insight into the effects of coordination by these two auxiliary ligands and also of the overall charge on the cyclometalated complex. For example, upon substituting isocyanide for cyanide in the series $Ir(ppy)_2(CN)_2^- \rightarrow Ir(ppy)_2(CN)(t\text{-BuNC}) \rightarrow Ir(tpy)_2(t\text{-BuNC})_2^+$, the quantum yield decreases from 0.94 to 0.67 to 0.28 while the luminescence lifetime increases from 3.1 to 14.0 to 35.6 μs, respectively. Furthermore, the calculated radiative rate constants decrease across this series: 30×10^4 to 4.8×10^4 to 0.78×10^4 s^{-1}. Previous studies[10] on the effect of ancillary ligands on the spectroscopic properties of cyclometalated Ir(III) complexes demonstrated that stabilization of the HOMO resulted in a decrease in ^{1}MLCT character in the emitting ^{3}LC state. This decrease in MLCT character is apparent across the present series, where the radiative rate constant decreases because of reduced spin−orbit coupling. Cyanide and isocyanide are both strong π-accepting ligands; therefore, the greater apparent stabilization of the HOMO across this series may be due, in part, to the higher positive charge on the complex that results from sequential coordination by isocyanide. The calculated nonradiative rate constants, however, are nearly equal at 1.9×10^4, 2.4×10^4, and 2.0×10^4 s^{-1}, respectively; therefore, the relative quantum yields are mostly dictated by the magnitude of the radiative rate constants.

However, the position of the first emission maximum does not follow a regular trend across the same series. The maximum for the most electron rich species $Ir(ppy)_2(CN)_2^-$ is furthest to the red at 470 nm. For neutral $Ir(ppy)_2(CN)(t\text{-BuNC})$, the maximum shifts to 458 nm, which is expected because of less electron density on the metal center, which stabilizes the HOMO. However, the emission maximum for cationic $Ir(tpy)_2(t\text{-BuNC})_2^+$ is unshifted (disregarding the minor influence of the methyl group) and also lies at 458 nm. This indicates a limit to the amount of blue shifting that is possible for these phenylpyridine complexes where the emission assumes predominately triplet intraligand character. The emissions of the mixed cyano−isocyanide complexes seem to lie right at that limit, while maintaining very high PL quantum yields.

Emission from Ir cyclometalates consists of varying degrees of MLCT character, which depends upon the identity of the cyclometalating and ancillary ligands. However, for analogous Rh complexes, the high oxidation potential of Rh moves the ^{1}MLCT states to very high energies,[27] and mixing with the emitting ^{3}LC state is always minimal. With coordination by the strongly electron withdrawing ancillary ligands cyanide and isocyanide, the oxidation potentials of the Ir complexes **1**−**6** grow large, and the spectroscopic properties begin to resemble those of Rh cyclometalates. For example, the first emission maxima, measured at 77 K, for $Rh(ppy)_3$, $Rh(ppy)_2(CN)_2^-$, and $[Rh(ppy)_2Cl]_2$ range from 460−464 nm, which are near to that of **1**. However, unlike the Rh complexes, **1**−**6** display very intense room-temperature PL. This difference can be understood by considering the inherent differences in second and third row transition metals. With a higher degree of spin−orbit coupling for Ir, relaxation from the T_1 state to the S_0 state is more allowed in these complexes than for those of Rh. Furthermore, the larger ligand field-splitting strength of Ir moves the dd states well above those of the emitting state.

Conclusions

A new family of bis-cyclometalated iridium complexes with both cyanide and isocyanide ancillary ligands were synthesized and structurally and photophysically characterized. The crystal structures of **3** and **6** reveal pseudo octahedral coordination geometry with the ancillary ligands trans to the cyclometalated phenyls. These complexes display deep blue PL while maintaining high quantum yield efficiency in deoxygenated solutions. A lack of solvatochromism, a highly structured emission, and the luminescent lifetimes of around 14−21 μs point to a ^{3}LC emitting state with a small admixture of ^{1}MLCT character.

The complexes are stable in solution and in air but thermally decompose with attempts to sublime. For example, **6** begins to decompose at 304 °C, thus, precluding thermal evaporation as a means of depositing films of this material

(24) (a) Coppo, P.; Plummer, E. A.; De Cola, L. *Chem. Commun.* **2004**, 1774−1775. (b) Mak, C. S. K.; Hayer, A.; Pascu, S. I.; Watkins, S. E.; Holmes, A. B.; Köhler, A.; Friend, R. H. *Chem. Commun.* **2005**, 4708−4710.

(25) Yeh, S.-J.; Chen, C.-T.; Song, Y.-H.; Chi, Y.; Ho, M.-H. *Journal of the Society for Information Display* **2005**, *13*, 857−862.

(26) Sajoto, T.; Djurovich, P. I.; Tamayo, A.; Yousufuddin, M.; Bau, R.; Thompson, M. E. *Inorg. Chem.* **2005**, *44*, 7992−8003.

(27) (a) Ohsawa, Y.; Sprouse, S.; King, K. A.; DeArmond, M. K.; Hanck, K. W.; Watts, R. J. *J. Phys. Chem.* **1987**, *91*, 1047−1054. (b) Colombo, M. G.; Hauser, A.; Güdel, H. U. *Top. Curr. Chem.* **1994**, *171*, 143−171.

for optoelectronic devices. However, attempts are underway to incorporate the new complexes in solution-processed OLEDs. Their high-energy phosphorescence, however, requires organic charge-transporting host materials with similarly high-energy triplet states in order to avoid quenching by triplet energy transfer to the host. Most optoelectronic applications of transition metal complexes employ neutral species; therefore, these mixed cyano−isocyanide complexes may find greater utility than their charged dicyano or diisocyanide counterparts.

The introduction of isocyanide ligands to Ir cyclometalated complexes affords new possibilities in adding functionality to materials. For example, the R group of isocyanide can be used as a point of attachment to polymers, nanoparticles, or biomolecules such as for phosphorescent biological tags.

Acknowledgment. The authors thank Dr. James Sumner for his kind assistance with the electrochemical measurements.

Supporting Information Available: Absorption spectra of **1**, **2**, and **3**, the emission spectra of $\mathbf{1}_{Cl}$, $\mathbf{2}_{Cl}$, and $\mathbf{3}_{Cl}$, and the CIF files of **3** and **6**. This material is available free of charge via the Internet at http://pubs.acs.org.

IC061513V